 doi:10.20944/preprints201801.0200.v1

Highly Efficient Step-Up Boost-Flyback Coupled Magnetic Integrated Converter for Photovoltaic Energy

Vu Thai Giang
Hanoi University of Industry, Hanoi, Vietnam
Vo Thanh Vinh
Hung Yen University of Technology and Education, Hung Yen, Vietnam
Nguyen The Vinh
Fac of Electrical, Quang Ninh University of Industry, Quang Ninh, Vietnam
E-mail vinhnt@qui.edu.vn

Abstract: - This paper presents a new high-efficiency-high-step-up based converter integrating two stype DC-DC Boost and Flyback coupled magnetic converter with recovery stage dedicated to smart HVDC distributed architecture in renewable energy production systems. Appropriate duty cycle ratio assumes that the recovery stage work with parallel charge and discharge to achieve high step-up voltage gain. Besides, the voltage stress on the main switch is reduced with a passive clamp circuit and thus, low on-state resistance Rdson of the main switch can be adopted to reduce conduction losses. The circuit is simple to control. As a final point of this research, the simulation and the prototype investigational results are presented to demonstrate the effectiveness of this proposed converter.

Key-Words: - DC-DC converters; boost converter; flyback converter; high step-up voltage gain; sustainable energy system

1 Introduction

At present the dependency on renewable energy sources are increasing day by day because of the energy deficiency and the environmental contamination caused by the fossil fuels. The major downside of renewable energy source is that it generates low voltage output. So the high step up DC-DC converter has been widely employed in many renewable energy applications [1-5]. The renewable energy system transfers energy from renewable sources to electrical energy and convert low voltage to high voltage by using a step up converter. Mainly DC boost and flyback converters are needed to boost up DC voltage.

In a recent publication [6-8], we have analyzed by simulation, modeled and tested a prototype of an original MCB converter with intermediary recovery stage (MCB-RS) having a single secondary stage dedicated to renewable energy conversion for middle power installation [7]. The recovery stage is a passive clamping circuit allowing the recovery of the energy lost in the leakage inductor and the clamping of the voltage in the switch. In the current contribution, we present a new step-up converter with two secondary stages developed to improve the voltage gain while limiting the voltage across the MOSFET. This converter is named Boost-Flyback with recovery stage (BF-RS) for magnetic coupled boost and flyback with recovery stage converter. Besides, the secondary-stage of the coupled inductor can alleviate the reverse-recovery problem of diodes rectifier, as present in the previous MCB-RS converter.

If the duty ratio is larger means the output voltage is high, but it leads to high conduction time and also that leads to resulting in high voltage stress on the switching device causes large conduction loss [9]. By the use of the interleaved boost converter with voltage BF-RS concept it will achieve high output voltage and reduce the voltage stress and conduction loss.

2 Research method general presentation BF-RS converter

Figure 1 shows the circuit topology of the proposed Boost-Flyback with recovery stage BF-RS converter. The BF-RS is based on a boost and flyback converter with one primary and two secondary coupled inductors, each secondary stage associated with its own energy storage capacitor, named C1, C2 and C3 in Figure 1. The switch is represented by a MOSFET M1, driven by a PWM signal generated to delivered the maximum possible power generated by the input variable energy source (from a photovoltaic panel, as example). The equivalent circuit model of the BF-RS converter includes the inductor L1 and the leakage inductor Lk1 of the primary coil, and the corresponding L2,

Preprints (www.preprints.org) | NOT PEER-REVIEWED | Posted: 22 January 2018 doi:10.20944/preprints201801.0200.v1

L3, Lk2 and Lk3 for the two secondary coils. The recovery stage is constitutes by the diode D1 and the capacitor C1 (Full explanation of the working modes of this recovery stage are fully described in Ref. [7]).

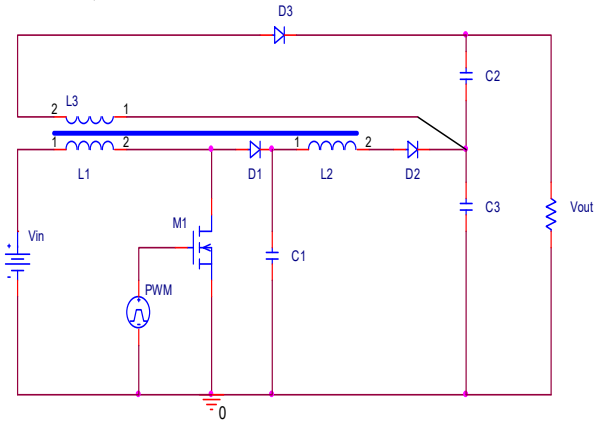

Figure 1. Diagram Boost-Flyback coupled magnetic of a converter with stage RS

As we can see, the architecture of the BF-RS converter remains quite simple with one switch, three diodes, three capacitors; the main elements being the interleave two secondary inductors, having adapted transformation or turn ratio. The turn ratio of the first coupled secondary inductor determines the voltage across the capacitor C3. The second secondary inductor allows a complementary adjustment of the total gain of the converter to the nominal voltage expected at the output of the converter. Within this architecture with both amplification levels, one can expect an additional significant decrease of the voltage across the MOSFET compared to basic converter and as a consequence a limitation of the losses due to the resistance Rdson, losses having a sub-linear proportionality to the voltage Vds [10]. Thus, compared to a basic boost and flyback converters, the BF-RS converter seems to be a simple solution to increase the efficiency while keeping a high output voltage. The output voltage concerns the continuous magnetic flux mode operation, i.e. the situation in which the energy stored in the choke at no point in time decreases to zero. As it results from the relationship [11], in comparison with a standard boost converter, the boost-flyback converter at the same duty cycle allows for obtaining higher voltage gain value, which additionally can be fixed by means of an appropriate selection of turns ratio in coupled choke. Moreover, in the boost-flyback converter, unlike in the flyback topology, no voltage spikes occur on the transistor. It is so because the energy stored in the choke primary winding leakage inductance is transferred to the output capacitor C1and C3. Hence, there is no need to use overvoltage protection elements.

3 Operation of converter

The operation principle of the proposed circuit can be explained with four modes:

3.1 Mode 1

In this mode of operation, the switches M1 is conducting on while the diodes D1, D2 and D3 are turned off which is exposed in Figure 2. The magnetizing inductor L1 stores its energy from the DC source V_{in}. Due to the leakage inductor of L1, the secondary-side current of the coupled inductor i_{L2} equals zero. The output voltage equals the voltage V_{out}.

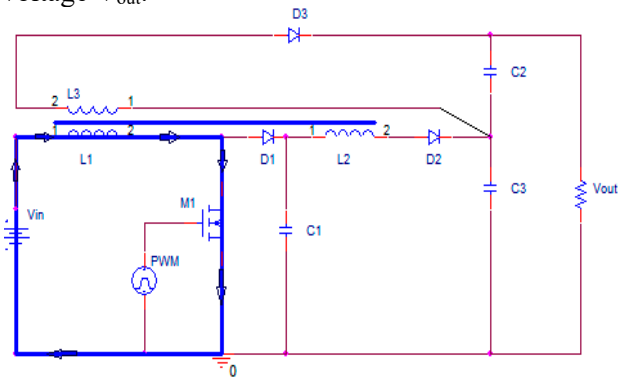

Figure 2. Mode 1 operation

3.2 Mode 2

The mode-2 operation is revealed in the Figure 3. In this mode, the switch M1 is turned off while diodes D1, D2 and D3 are turned on. The primary-side current of the coupled inductor iLk1 linearly decreases. The energies of the leakage inductor of L1 and magnetizing inductor L1 are released to the clamp capacitor C1. The primary and secondary windings of the coupled inductor, DC sources V_{in}, transfer their energies to the output load path followed by the induced energy will be L2–D2–L3 – D3. In which, the capacitor C2 is still charge and more slowly than C3.

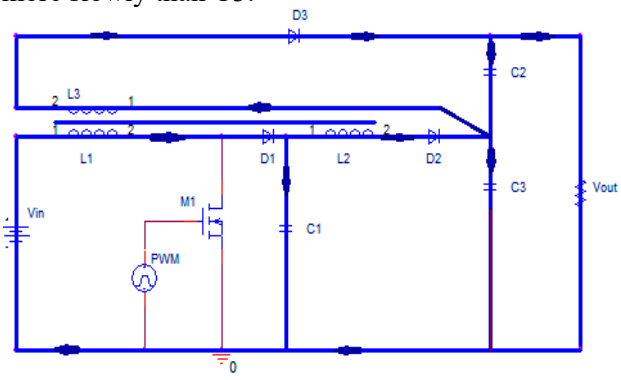

Figure 3. Operation of converter at the mode 2

3.3 Mode 3

The mode 3 operation is shown in the Figure 4. The switch M1 and D1 are turned off and diodes D2 and D3 are turned on. The primary-side current of

Preprints (www.preprints.org) | NOT PEER-REVIEWED | Posted: 22 January 2018 doi:10.20944/preprints201801.0200.v1

the coupled leakage inductor iLk1 is continuously linearly decreasing but at a slower rate than mode 2. The primary-side and secondary-side windings of the coupled inductor, DC sources Vin, and clamp capacitor C1 transfer their energies to the load follow by part C1-D2-D3. The capacitor C2 and C3 is still charge by capacitor C1. In this mode also both the diodes D2 and D3 are conducting. The energy is stored bythe coupled inductor. Along with the self-inductance, the occurrence of the mutual inductance also takes place and due to this the output value is increased.

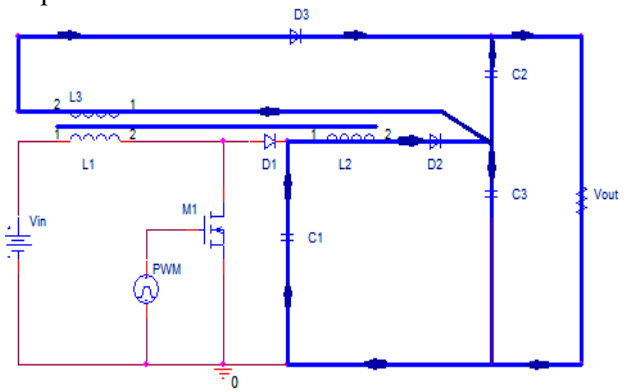

Figure 4. Mode 3 operation

3.4 Mode 4

The switch M1, D1 and D2 are turned off and D3 is turned on. The primary-side current of the coupling inductor equals zero. Beside, the secondary L2 current equals zero reason the capacitor C1 is discharge. Clamp capacitor C2 and C3 transfers their energy to the load, the path followed by the induced energy will be C3– L3 –D3.

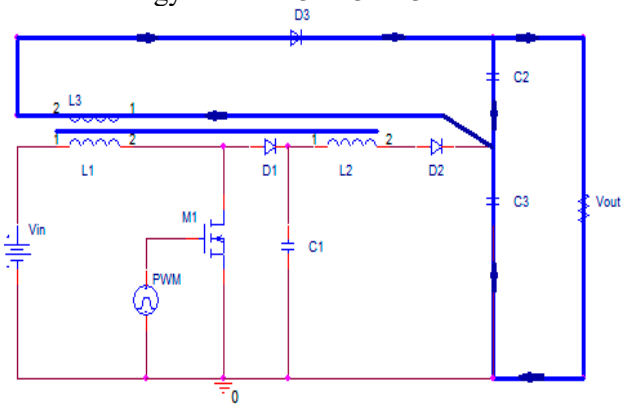

Figure 5. Mode 4 operation

4 Resilts and discussion

4.1 Simulation results

The input voltage is givenin the simulation of the proposed circuit is 20V which is shown in the Figure 6. The output voltage achieved in the simulation is 317V which is shown in the Figure 7. The diagram simulated of the laboratory prototype is shown in Figure 6. Each block of the laboratory prototype is explained as follows. DC source gives the DC supply to the converter. The DC source from panner solar. This output has ripples. It is filtered with thehelp of Capacitor. The load is the resistor. PIC 16F876A microcontroller is used to generate triggering pulse for MOSFET. It is used to control the outputs. Microcontrollers have more advantages such as fast response, low cost, small size and etc. Interleaved boost-flyback converter low voltage dc supply to high voltage DC supply. The output voltage is controlled by controlling the firing angle of the MOSFET and transformation ratio. The driver arealso called as power amplifier andthey are used to amplify the pulse output from microcontroller. It is also called as driver IC. It provides isolation between microcontroller and power circuits.

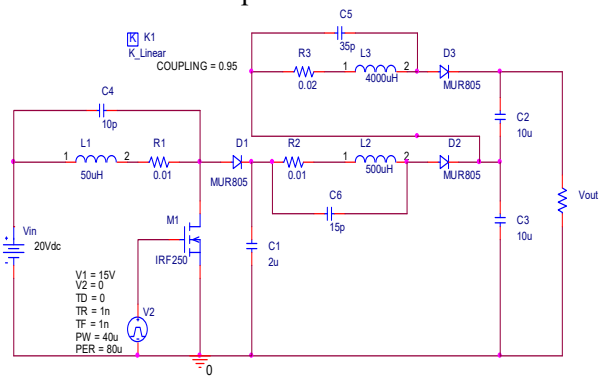

Figure 6. Simulation Boost-Flyback coupling magnetic-recovery stage

All the inductors, i.e. L1 for the primary and L2 and L3 for the two secondary stages are represented with their respective resistors, R1, R2 and R3, and their respective parasitic capacitors C4, C5 and C6. We have chosen a realistic value for the coupling factor equal to 0.95, currently achieved in practice.

For the modeling of the behavior of the converter, we have chosen setup with same amplification ratio for the two stages, i.e. a setup having secondary windings, L3 = 4*L2 for the stype Boost and Flyback converter. To reduce the voltage stress on the M1 and D2 that the high output voltage in the proposed converter as Figure 7.

The voltage shapes in Figre 7 show clearly the energy recovery phase show the curves of voltage VC1 of C1 (line violet) followed by RS stage. The stage in turn the energy recovery leaking primary winding, corresponding to the ratio of transformation by effect of the magnetic Boost to increase performance for this converter. Add the voltage on M1 is improved to reduce by dividing the secondary windings of the transformerwhen the low value as 0.7 of the coupling coefficient previously generated high voltage, the voltage on the transistor does not exceed the maximum permissible value, which ensures its protection.

Preprints (www.preprints.org) | NOT PEER-REVIEWED | Posted: 22 January 2018 doi:10.20944/preprints201801.0200.v1

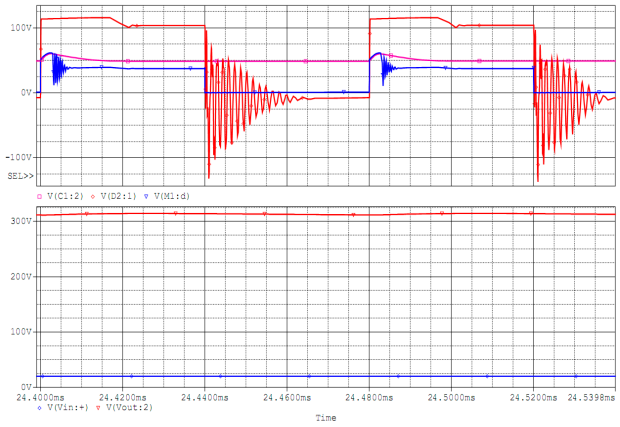

Figure 7. Simulated input and output voltage, voltage stress rectifier of the diodes D2 of the converter. For this simulation, the transformation ratio is fixed at a standard value duty ratio = 0,5, k=0.95

4.2 Experimental module

In Figure 8 we show the corresponding picture of the laboratory prototype used for the tests. In order to conduct tests in conditions similar to actual conditions. However, majority of the laboratory tests were conducted with the use of a the resistance load. Additionally, on the input to the DC-DC converter, a capacitor filtering the converter current (containing a considerable AC component) was placed. Figure 8 shows a photo of the test bed.

The waveforms from the DC-DC converter system operation with resistance load (R_L = 274 Ω) are shown in Figure 9.

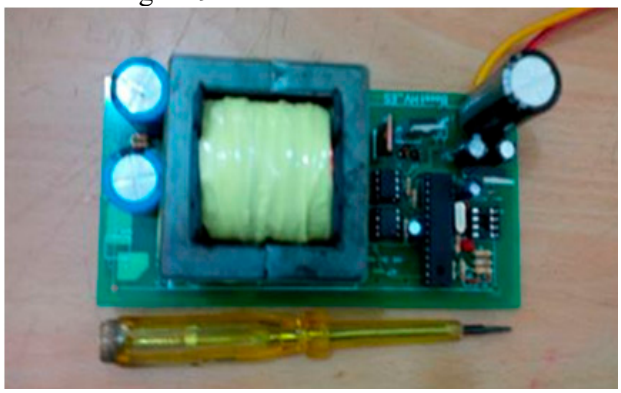

Figure 8. Hardware picture of the proposed converter

As part of the laboratory works, the boost-flyback with the recovery stage output voltage and duty ratio characteristic curves were measured, loaded with the resistance R_L = 274 Ω. The value of the input voltage was fixed at 20V. The output voltage was determined as the sum of the voltages measured on both output capacitors C2 and C3 as Figure 6. The output voltage characteristics dependent duty cycle, transformation ratio and ratio between two inductors L2, L3 function various choke are shown in Figure 6.

It should be noted that the valer of the inductors L2, L3 (hence the choke parasitic parameters value) has significant influence on the flyback converter voltage, and it has influence on the value of the boost converter output voltage. This leads, influence direct the voltage stress on the MOSFET, Diode of the converter. The influence of the choke parasitic elements becomes more important as the duty cycle increases.

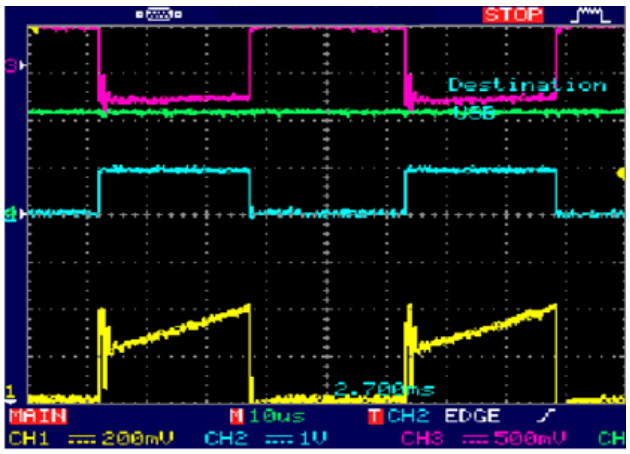

Figure 9. The waveforms: Current of the MOSFET (line yellow); Pulse wide modifier driver (line blue); Voltage on the D2 (line violet); Voltage on the capacitor C1 in the circuit recovery stage (line green)

5 Conclusion

The paper presents the DC-DC BF-RS converter enabling the adjustment of the photovoltaic panel output voltage (25÷60)V. The use of this typology allows for obtaining high voltage gain coefficients at relatively low duty ratio (in relation to the boost converter). In comparison with other solutions, alternative to the conventional boost and flyback converter, the converter is composed of a small number of elements. Moreover, it can operate with a choke of low inductance value (despite the operating mode, the input current contains a high variable component). With appropriate selection of turns ratio two secondery inductor, it is possible to limit the MOSFET transistor operating voltage value and boost converter diode operating low voltage. As a result, the losses in the BF-RS converter circuit decrease. This converter architecture may be a track in the development of the distributed architecture of HVDC bus.

ACKNOWLEDGEMENTS

The authors gratefully acknowledge the Hanoi University of industry, Dong Thap University, Quang Ninh University of industry for the

financially support and for the facilities offered during these researches. This research was supported by Center for Research and Applications in Science and Technology, Hung Yen University of Technology and Education, under grant number UTEHY.T013.P1617.02.

References:

[1] RG Walker and PC Sernia., "Cascaded DC–DC Converter Connection of Photovoltaic Modules," *IEEE Trans. on Power Electron.* Vol.8, 4, pp 1130-1139, 2004.

[2] A Shahin *et al*., "New non-linear control strategy for non-isolated DC/DC converter with high voltage ratio," *Energy Conversion and Management*. Vol.51, 1, pp56-63, 2010.

[3] Tseng K.C., Liang T.J., "Novel high-efficiency step-up converter," *Proc. Inst. Elect. Eng. Elect. Power Appl*. Vol.151, 2, pp182-190, 2004.

[4] Li W, He X., "Review of nonisolated high-step-up DC/DC converters in photovoltaic grid-connected applications," *IEEE Trans. Ind. Electron.* Vol.58, 4, pp1239-1250, 2011.

[5] F.L. Luo, "Switched-capacitorized DC/DC converters" *in Proc. IEEE c\Conf. Ind. Electron. Appl. (ICIEA),* pp. 1074-1079, 2009.

[6] Q Zhao, FC Lee., "High-Efficiency High Step-Up DC–DC Converters,". *IEEE Trans. Power Electron.* Vol.18, 1, 2003.

[7] Nguyen The Vinh *et al.,* "Efficiency of magnetic coupled boost DC-DC converters mainly dedicated to renewable energy systems: Influence of the coupling factor," *International Journal of Circuit Theory and Applications*, Vol. 43, pp1042–1062, 2014.

[8] T.V. Nguyen *et al.*, "Self-powered High Efficiency Coupled Inductor Boost Converter for Photovoltaic Energy Conversion," *Energy Procedia*, Vol.36, pp650-656, 2013.

[9] Pierre Petit *et al.,* "Basic MOSFET Based vs Couple-Coils Boost Converters for Photovoltaic Generators," *International Journal of Power Electronics and Drive Systems*, Vol.4, 1, pp1-11, March 2014.

[10] P. Petit *et al.,* "Rdson behavior in various MOSFET families," *IEEE IndustrialElectronics ISIE*, pp353 – 357, 2011.

[11] Adam Kawa *et al.,* "DC-DC boost-flyback converter functioning as input stage for one phase low power grid-connected inverter," *Archives of electrical engineering*, Vol. 63, 3, pp393-407, 2014.